Production of an Asparaginase-Like Domain of AnsA from *Methanocaldococcus jannaschii* in *Escherichia coli*, its purification and *In Silico* Analysis

Maham Ijaz, Mohsin Shad, Arshia Nazir, Naseema Azim and Muhammad Sajjad*

School of Biological Sciences, University of the Punjab, Lahore, 54590, Pakistan

ABSTRACT

L-asparaginase (E.C 3.5.1.1) is a highly valuable enzyme owing to its ability to function as a chemotherapeutic agent against certain lymphomas such as acute lymphoblastic leukemia. This enzyme also mitigates the level of acrylamide production in processed food items. L-asparaginase performs the two-step hydrolytic reaction that results in the deamination of amino acid asparagine into aspartic acid and ammonia. L-asparaginases are widely distributed in three domains of life but their microbial source is getting much attention in the field of pharmaceutical industry due to cost effectiveness and ease of production. The focus of current research work is the utilization of various *in silico* tools for structural and functional analysis of an asparaginase-like domain of *ans*A gene from *Methanocaldococcus* sp. The DNA fragment coding for the asparaginase-like domain was PCR amplified, cloned, and expressed using recombinant DNA technology. Specifically designed primers were used for PCR amplification of *ans*A(T) gene from the genomic DNA of *M. jannaschii* DSM 2661. After PCR amplification, the gene was first cloned into the cloning vector (pJET1.2/blunt) and thereafter cloned in expression vector pET-28a (+). *E. coli* BL21 CodonPlus (DE3)-RIL was used as an expression host to produce an asparaginase-like protein, AnsA(T). The recombinant protein AnsA(T) was expressed in soluble form in *E. coli*. Moreover, the thermostability of the enzyme was determined by heating the supernatant at different temperatures ranging from 60-90 °C for different durations of time. Additionally, the AnsA(T) enzyme was partially purified by heat treatment at 80 °C for 15 min followed by Ni-NTA chromatography. The highly thermostable asparaginase AnsA(T) of *Methanocaldococcus* sp. can make it a potential candidate for its applications in the food industry.

INTRODUCTION

L-asparaginase (L-ASNase), an amidohydrolase (E.C 3.5.1.1) that performs the hydrolytic reaction resulting in the conversion of L-asparagine into the products, aspartate and ammonia (Chi *et al.*, 2022). Based on structural similarity and biochemical properties, L-asparaginases come under 3 classes: Bacterial type (class 1, type I and II), plant-type (class 2, type III) and third class involved *Rhizobium etli*-type (type IV) (Loch and Jaskolski, 2021). The bacterial L-asparaginases are classified into two main types: type I and type II L-asparaginases. Type I L-asparaginases are cytosolic enzymes that exhibit low substrate affinity and show low to high glutaminase activity. Type II L-asparaginases, also abbreviated as *EcII* are periplasmic enzymes that display low K_m values towards L-asparagine and low glutaminase activity (Zielezinski *et al.*, 2022). Pant-type (type III) L-asparaginases belong to the N-terminal nucleophile hydrolase family (Gabriel *et al.*, 2012). The enzyme is synthesized as a single inactive polypeptide precursor that exists in the form of a mature heterodimer $(\alpha/\beta)_2$ of two subunits that display activity when undergoes autoproteolytic cleavage to form alpha and beta subunits. Plant L-asparaginases are classified into K$^+$-dependent and K$^+$-independent L-ASNases depending on their requirement for potassium ions for catalysis (Sajed *et al.*, 2022). The enzyme finds its application in both the pharmaceutical and food industries.

The hydrolytic process performed by L-ASNase inhibits the proliferation of cancerous cells by depleting the presence of L-asparagine in blood plasma, which is

an essential nutrient for the growth of malignant cells (Naz *et al*., 2021). Additionally, the thermostability of L-ASNase enables its use in industrial applications including acrylamide mitigation in fried and baked food items (Sajed *et al*., 2022). Acrylamide is formed as a side product when asparagine reacts with reducing sugar in the Maillard reaction (Munir *et al*., 2019). Thus, converting asparagine to aspartic acid before baking mitigates acrylamide production. The stability of an enzyme is a crucial aspect that influences its suitability for industrial or therapeutic uses. L-ASNase is also a thermostable enzyme isolated from hyperthermophilic sources. Several highly stable L-asparaginases have also been reported from extremophilic origin such as *Pyrococcus yayanosii* (Li *et al*., 2018), *Pyrococcus abyssi* (Nadeem *et al*., 2021), *Pyrobaculum calidifontis* (Chohan *et al*., 2019), *Pyrococcus horikoshii* (Yao *et al*., 2005), *Pyrococcus furiosus* (Saeed *et al*., 2020), *Thermococcus kodakarensis* (Hong *et al*., 2014), *Thermococcus gammatolerans* (Zuo *et al*., 2014), *Thermococcus zellige* (Zuo *et al*., 2015), *Archaeoglobus fulgidu* (Li *et al*., 2002). *Methanocaldococcus jannaschii* is an autotrophic hyperthermophilic archaeon phylogenetically associated with the kingdom Euryarchaeota that grows optimally at 85 °C (Malandrin *et al*., 1999; Susanti *et al*., 2019). The genome of *M. jannaschii* reveals an open reading frame for the *ans*A gene that has an asparaginase-like domain. For the current study, truncation of this asparaginase (*ans*A) gene was made based on the theoretically determined parameters and sequence homology of domains. The physicochemical properties, molecular modelling, cloning of the asparaginase gene in an expression vector, and its downstream processing were comprehensively explored in this research work.

MATERIALS AND METHODS

Reagents, plasmids, and strains

All the chemicals used in this study were of reagent grade. CloneJET PCR Cloning Kit, GeneJet Gel extraction kit, GeneRuler™ DNA ladder mix (SM0331), Protein Ladder (cat. #26614) and PageRuler™ protein ladder (SM0671) were purchased from Thermo Fisher Scientific. Restriction enzymes *Nde*I (cat. #ER0582) and *Xho*I (cat. #ER0691), RNase A, and T4 DNA ligase were also bought from Thermo Scientific, USA. Acrylamide was purchased from Fluka™ and Bis-acrylamide from Acros Organics™. Primers were commercially synthesized by Humanizing Genomics; (Macrogen Inc., Seoul, The Republic of Korea). *E. coli* strains (DH5α™ and BL21CodonPlus (DE3)-RIL) and pET-28a (+) were from Novagen (Merck, Germany).

Cloning of ansA(T) gene

The asparaginase-like domain of *ans*A gene (1038 bp) was PCR amplified using genomic DNA of *M. jannaschii* as a template, and gene-specific forward (5′-CAT-ATGTTAAAAACAATCTCTATTTTATCCAC-3′) and reverse (5′-CTCGAGGTATGCATCAAATCTGCTC-3′) primers. Restriction sites for *Nde*I and *Xho*I were inserted at the 5′-ends of forward and reverse primers, respectively (underline sequences). The purified amplicon was ligated into the pJET1.2 cloning vector in a 3:1 molar ratio by using T4 DNA ligase. The presence and orientation of the inserted gene in the recombinant plasmid were first screened through colony PCR of transformants and then further confirmed by performing restriction digestion analysis. The presence of any PCR-related unwanted mutation was confirmed through Sanger's DNA sequencing. After successful cloning and confirmation of the *ans*A(T) gene in the cloning vector, the insert was sub-cloned into expression vector pET-28a (+) using *Nde*I-*Xho*I restriction sites. The confirmed recombinant construct pJET1.2_*ans*A(T) was digested using the same set of restriction endonucleases (*Nde*I-*Xho*I) and ligated into the pET-28a (+) expression vector.

Heterologous production of recombinant AnsA(T)

The resulting recombinant construct pET28a_*ans*A(T) was used for the heterologous production of recombinant AnsA(T) in *E. coli* BL21 CodonPlus (DE3)-RIL cells. The cells were induced with 0.5 mM IPTG (final concentration) and 4 h of post-induction time was given at 37 °C when the optical density at 600 nm reached 0.4-0.5. The cells were subjected to centrifugation at 6000 *x g* at 4 °C for 10 min. The 2g cell pellet was washed and resuspended in 25 ml of 50 mM Tris-Cl buffer (pH:8.0). Cells were sonicated for lysis by using the Bendelin SonoPlus HD 2070 sonication system. Centrifugation (15,000 *xg* for 15 min) was performed to separate soluble and insoluble fractions. Negative control was prepared by using the sample in which the cells contained only pET-28a (+) vector also induced with 0.5 mM IPTG. All the fractions were collected and analyzed by 12% polyacrylamide gel electrophoresis (SDS-PAGE).

Heat treatment optimization of AnsA(T)

As the AnsA(T) enzyme is from a thermostable source, the sonic supernatant was heated at different degrees of temperatures, i.e., 60, 70, 80, 85 and 90 °C for 15 and 30 min at each heating temperature. Soluble and heat-precipitated proteins were separated by centrifugation and analyzed on 12% SDS-PAGE for comparison through the gel documentation system (Javaid *et al*., 2022).

Purification of recombinant AnsA(T)

Cells were lysed to extract the proteins and sonic supernatant was partially purified by heating at 80 °C for 15 min. A heated fraction of recombinant AnsA(T) protein was used for further purification through Ni-NTA chromatography as the recombinant protein contains a 6X-His tag at its both termini (Shad *et al.*, 2024). Fractions were collected at different gradients of imidazole, i.e.,150, 200, 250, 300, 350 and 400 mM. SDS-PAGE analysis was performed to check the purity of protein in eluted fractions following the method described by (Chi *et al.*, 2023). Selected fractions containing AnsA(T) were pooled for dialysis. Protein was dialyzed initially against 50 mM Tris-Cl buffer (pH:8.0) containing 100 mM NaCl and 5 mM EDTA. Dialysis was repeated with the same buffer without EDTA (Arif *et al.*, 2022).

Sequence and structure analysis of AnsA(T)

The 3D structure of the asparaginase-like domain was predicted by using the online modelling program phyre2 (http://www.sbg.bio.ic.ac.uk/phyre2/html/page.cgi?id=index). The overall quality factor of the 3D model for non-bonded atomic interactions was assessed through an ERRAT server (https://servicesn.mbi.ucla.edu/ERRAT/) (Shad *et al.*, 2023). The various physicochemical properties and amino acid composition of AnsA(T) protein were computationally calculated by the ExPASy ProtParam tool (https://web.expasy.org/cgi-bin/protparam/protparam). Multiple sequence alignment of the AnsA(T) domain was performed using computer-aided software, Clustal Omega (https://www.ebi.ac.uk/Tools/msa/clustalo/) with its homologues of hyperthermophilic archaeal and bacterial asparaginases. The predicted structure of the asparaginase-like domain was superimposed with the crystal structure of *P. horikoshii* (PDB ID:1WNF) by using PyMol (Shad *et al.*, 2023) (https://pymol.org/2/).

RESULTS

Molecular cloning of ans*A(T) gene into an expression vector*

The polymerase chain reaction of the *ans*A(T) gene was performed using a set of gene-specific primers and genomic DNA of *M. jannaschii* as a template, which resulted in the amplification of the required band of about 1.0 kb (Fig. 1A). Gel-purified PCR amplicon of *ans*A(T) was cloned through blunt end cloning in pJET1.2 (Fig. 1B). Colony PCR of *E. coli* DH5α colonies containing recombinant plasmid pJET1.2_*ans*A(T) indicated the three colonies showing a band of 1038 bp which confirmed the presence of *ans*A(T) in pJET1.2 (Fig. 1C). Double digestion utilizing *Nde*I and *Xho*I resulted in the excision

of two DNA fragments at the positions of ~1.0 kb and 2.97 kb also confirming the presence of the *ans*A(T) gene. The restricted purified gene was sub-cloned in expression vector pET28a (+) (Fig. 1D). Screening through colony PCR showed the presence of three colonies of *E. coli* DH5α transformed with recombinant plasmid pET28a_*ans*A(T) as shown in Figure 1D. Double digestion analysis using the same set of endonucleases (*Nde*I and *Xho*I) also confirmed the presence of insert as shown in Figure 1E.
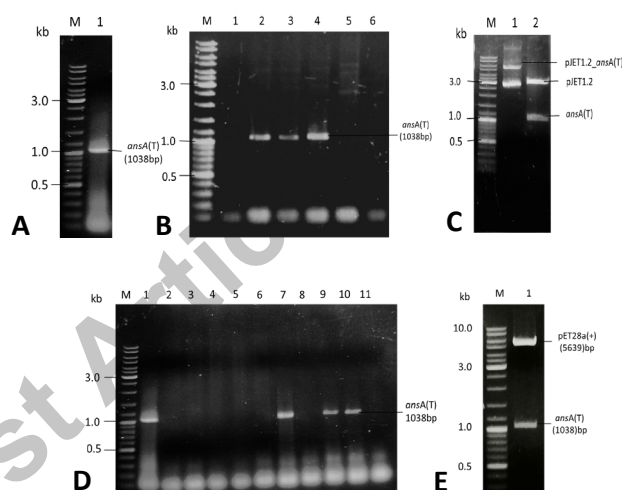

Fig. 1. 1% agarose gel stained with ethidium bromide demonstrating the cloning of *ans*A gene. (A)PCR amplified band of *ans*A(T). Lane M, DNA marker; Lane 1: amplified *ans*A(T) gene band of 1kb. (B)Positive pJET1.2_*ans*A(T) transformants by colony PCR. Lane M: DNA marker; Lane 1: Negative control; Lane 2: Positive control; Lane 4-9: Colony PCR of amplified gene bands of ~1.0 kb from colonies of pJET1.2_*ans*A(T) transformants. (C) Double digestion of pJET1.2_*ans*A(T) with *Nde*1 and *Xho*1. Lane M, DNA marker; Lane 1, unrestricted recombinant plasmid pJET1.2_*ans*A(T), Lane 2, two restricted fragments (2973 bp and 1038 bp). (D) Positive pET-28a_*ans*A(T) transformants by colony PCR. Lane M: DNA marker; Lane 1: Positive control; Lane 2: Negative control; Lane 3-11: Colony PCR of transformed colonies. (E) Restriction analysis of recombinant pET28a_*ans*A(T) plasmid. Lane 1, DNA marker; Lane 2, *Nde*1-*Xho*1 digested pET28a_*ans*A(T).

Expression of recombinant ans*A(T) gene*

Expression of cloned gene by giving induction of 0.5 mM IPTG for 4 hours using *E. coli* BL21 CodonPlus (DE3)-RIL demonstrated the production of recombinant protein at a size of about thirty-eight kDa as shown in Figure 2. Analysis of the different fractions of total cell lysate showed that most of the expression was in supernatant indicating its soluble expression (Fig. 2).
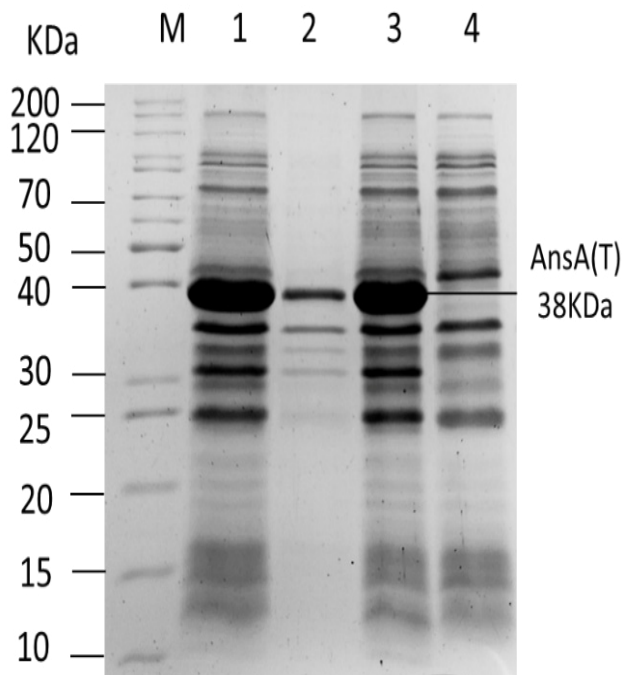
Fig. 2. Coomassie brilliant blue stained 12% SDS gel displaying the expression of pET28a_ *ans*A(T) with 0.1 mM IPTG induction and expression of the protein in the negative control, i.e., pET-28a (+) transformed *E. coli* BL21 cells. Lane M: Unstained Protein Ladder; Lane 1: total cell lysate from induced pET-28a_*ans*A(T); Lane 2: insoluble fraction from induced cells; Lane 3: soluble fraction from induced cells; Lane 4: total cell lysate from induced cells of pET-28a(+).
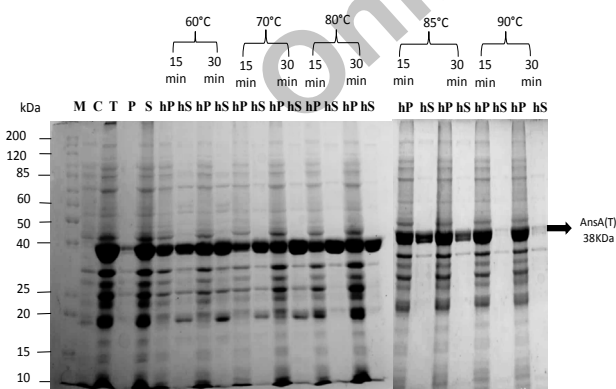

Fig. 3. Optimization of heat treatment of supernatant of *E. coli* BL21-pET-28a_*ans*A(T). Lane M: Unstained Protein Ladder, C: pET28a(+) control; T: total cell lysate; P: insoluble fraction; S: Soluble fraction; Lanes 6-25: hP (Heated pellet) and hS (Heated supernatant) at different degree of temperature (60, 70, 80, 85, 90) for 15 and 30 min, respectively.

Purification of recombinant enzyme through Ni-chromatography

The soluble fraction of recombinant AnsA(T) protein heated at different degrees of temperatures, i.e., 60, 70, 80, 85 and 90 °C for 15 and 30 min showed that the protein is stable up to 85 °C for 30 min (Fig. 3). But the temperature optimized for protein was 80 °C for 15 min at which most of the *E. coli* proteins are precipitated with no loss of AnsA(T) domain. A heated fraction of recombinant AnsA(T) protein with 6X-His tag was further purified through Ni-NTA chromatography. Analysis of the purity of different fractions collected at different gradients of imidazole showed that the protein was eluted between 200-350 mM concentration of imidazole (Fig. 4).
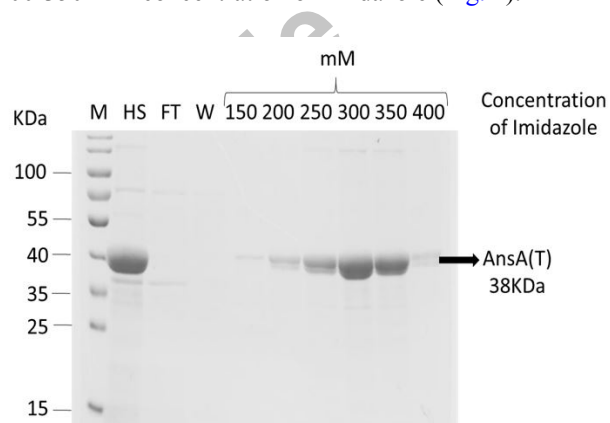

Fig. 4. 12% SDS PAGE showing purification of AnsA(T) protein through Ni^{+2} affinity chromatography L1; Protein Marker, L2; Heated Supernatant(hS), L3; Flow through(FT), L4; Wash (W) L (6-9); eluted fractions of AnsA(T) protein at 200, 250, 300, 350 mM concentration of Imidazole.

In silico sequence and structural analysis of ans*A(T) gene*

The genome of *M. jannaschii* has an open reading frame annotated as *ans*A gene having accession ID >AAB97996.1; with the position in the genome between 21148-22401. Asparaginase (AnsA) has three domains, N-terminal GatD domain as shown in green color followed by asparaginase N-terminal superfamily (sf) domain ad asparaginase C-terminal domain as predicted by NCBI Conserved Domain Database (Fig. 5A). Phyre2 was used to build the 3D model of the AnsA(T) domain (Fig. 5B). A 3D model was further validated through the ERRAT tool. Yellow areas on the structure indicate regions that can be rejected at a 95% confidence level; 5 percent of a decent protein structure is anticipated to have an error value above this threshold. Red indicates regions that are rejectable at a 99% confidence level as shown in Figure 6A. Ramachandran plot analyses performed through
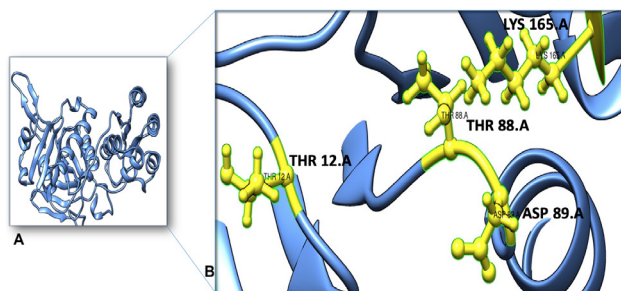
Fig. 5. (A) The schematic diagram for the position of different domains of asparaginase (AnsA). (B) The tertiary structure model of the AnsA(T) domain of asparaginase was predicted using Phyre2 and visualized using the PyMOL. The ribbon model of the AnsA(T) domain was labelled with cornflower colour. The 3D structure shows the predicted conserved active site of the AnsA(T) domain by COACH. Thr 12, Thr 88, Asp 89 and Lys 165 are predicted catalytic residues. The catalytic residues were shown in the ball and sticks model.
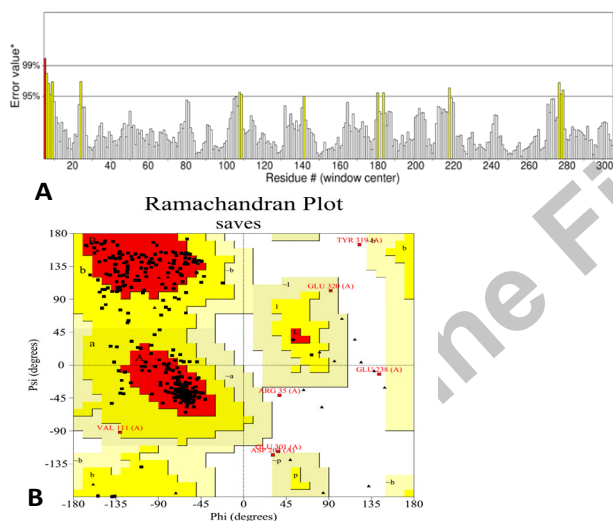

Fig. 6. (A), Assessment of overall quality factor of 3D model of AnsA(T) domain of *M. jannaschii* through ERRAT. Yellow areas on the structure indicate regions that can be rejected at a 95% confidence level; 5 percent of a decent protein structure is anticipated to have an error value above this threshold. Red indicates regions that are rejectable at a 99 percent confidence level. (B), Validation of a 3D model of AnsA(T) domain from *M. jannaschii* through Ramachandran plot. The most favored region is highlighted in red color. (A, B, L). Additional allowed regions are highlighted in yellow color (a, b, l, p). Generally allowed region is shown in light yellow colour (~a, ~b, ~l, ~p). The Ramachandran plot was made using the PROCHECK tool.

PROCHECK predicted that 79% of residues are in the most favored region, 18.7% residues in the additional allowed region, 1.0% in the generously allowed region

and 1.3% in the disallowed region as shown in Figure 6B. Results computed from the ExPASy tool, ProtParam predict that it has a theoretical isoelectric point of 6.46 with a molecular weight of 38252.16 Daltons. Multiple sequence alignment revealed the presence of all three conserved regions in asparaginase-like domain that are specific to Type-1 L-asparaginases of bacteria and archaea (Fig. 7). Superimposed 3D Crystal structure of *P. horikoshii* (PDB:1WNF) and AnsA(T) domain model created by phyre2 showed the conserved catalytic residues at exactly aligned positions in structures of both proteins except a slight difference in the spatial arrangement of Thr-12 residue (RMSD is 1.245 ºA) as shown in Figure 8.
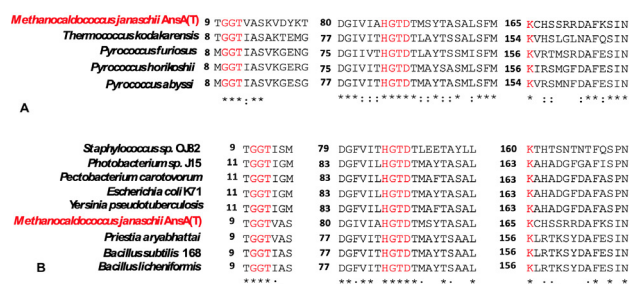

Fig. 7. Partial amino acid sequence alignment of the conserved regions of L-asparaginases from other characterized archaea and bacteria and AnsA(T) domain from *M. jannaschii*. The conserved catalytic residues of active sites are highlighted in a red colour. (A) Archaeal sources of the enzyme with their accession numbers are as follows: *Thermococcus kodakarensis* (WP_011250607.1), *Pyrococcus furiosus* (AAL82171.1), *Pyrococcus horikoshii*(WP_010884185.1), *Pyrococcus abyssi* (WP_048146476.1) (B). The organism's name with accession numbers of protein sequence from bacteria are as follows: *Staphylococcus* sp. (EJX17308.1), *Photobacterium sp.* (AIQ82557.1), *Pectobacterium carotovorum* (AFA36648.1), *Escherichia coli* K71(KRR58951.1)*, Yersinia pseudotuberculosis* (CFU95881.1), *Priestia aryabhattai*(KM000292.1)*, Bacillus subtilis* 168(NP_390239.1), *Bacillus licheniformis* (ARW56273.1).

DISCUSSION

Mesophilic sources of L-asparaginases exhibit low stability and are relatively less favorable than their thermophilic counterparts in meeting the challenging needs of this crucial enzyme in industrial applications (Dumina and Zhgun, 2023). Therefore, in the present experimental study, in *silico* analysis, cloning, recombinant production in *E. coli*, and purification of this asparaginase-like domain of asparaginase (AnsA) from hyperthermophilic archaeon *M. jannaschii* were performed with the idea that it will
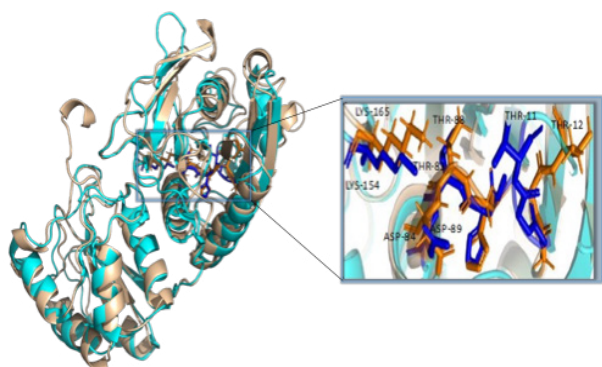
Fig. 8. Superimposition of the AnsA(T) domain from *M. jannaschii* (wheat) and L-asparaginase from *P. horikoshii* (PDB code: 1WNF) (cyan) showing the conserved active site and binding residues. Conserved motifs (GGT, HGTD) and catalytic residues (Thr-12, Thr-88, Asp-89, Lys165) of AnsA(T) domain from *M. jannaschii* are shown in sticks and ball model (orange) while catalytic residues (Thr-11, Thr-83, Asp-84, Lys-154) of L-asparaginase from *P. horikoshii* is shown in blue sticks and ball model.

be inherently stable. Thermophilic enzymes have a broad range of industrial applications because of their thermal stability and higher activity. The thermostability of an enzyme depends upon the composition and hydrophobicity of amino acids. This trait results from their unique structural characteristics, which are generally absent in proteins from mesophilic sources (Panja *et al.*, 2015).

A statistical analysis of preferred amino acids and the thermostability of enzymes has been reported. The abundance of five amino acid residues Ala, Gly, Val, Glu and Lys are favored in most thermostable proteins whereas non-preferred residues are Cys, His and Gln. (Farias and Bonato, 2003). By sequence analysis of the AnsA(T) domain, we found a higher percentage of hydrophobic residues such as Ala (7.2%), Gly (7.2%), Val (9.6%), Glu (8.4%) and Lys (8.7%) whereas the low content of thermolabile residues e.g. Cys (3%), Gln (4%) and His (7%) in the sequence. The genome sequence analysis showed that the hyperthermophilic archaeon *M. jannaschii* contains an open reading frame, *ans*A, encoding asparaginase. Domain analysis of asparaginase (AnsA) by Pfam and CDD of NCBI predicted the presence of three domains, 80 residues in the N-terminal specifically predicted as GatD amidotransferase domain, one in the center with only asparaginase domain and one involving center and C-terminal domain predicted the glutaminase /asparaginase domain with 28.5% sequence homology to *Pyrococcus furiosus* (PDB ID:5B74).

Several archaeal L-asparaginases showed structure similarity and sequence homology to eukaryotic and mesophilic bacteria (Lubkowski and Wlodawer, 2021). Therefore, the AnsA(T) domain was compared to the L-asparaginases present in hyperthermophilic bacteria and observed that the AnsA(T) domain was more like its archaeal than its bacterial counterparts. It showed 31% identities to both characterized archaeal counterparts from *Pyrococcus abyssi* and *Pyrococcus horikoshii*. More than 20% identity was also found with characterized bacterial counterparts from *Bacillus licheniformis*, *Escherichia coli* and *Pectobacterium carotovorum*. The alignment showed the conservation of catalytic residues that could be a sign of an evolutionary link between the two distinct domains of life.

Gene-specific primers were designed for the asparaginase-like domain and the gene was amplified by PCR using *M. jannaschii* genomic DNA as a template. The purified amplicon was cloned in the pJET1.2 cloning vector and screened by colony PCR and double restriction digestion. The gene was excised from the cloning vector and ligated into the expression vector pET-28a (+) (Bansal *et al.*, 2010). After the subsequent cloning confirmation, the recombinant construct produced was then transformed into *E. coli* BL21-CodonPlus competent cells via heat shock method to obtain the expression of the proteins similarly reported in (Dumina *et al.*, 2023). These transformed cells were then grown in the selective medium containing the antibiotic kanamycin similarly described by (Dobryakova *et al.*, 2023).

A solubility test was also performed to confirm the protein's nature. SDS PAGE analysis of soluble and insoluble fractions of total cell lysate after sonication indicated the soluble expression of recombinant protein as reported by (Chohan and Rashid, 2018). The AnsA(T) protein expression was optimized with IPTG concentrations and the induction time to obtain the optimal results of large-scale production. The best results were obtained in the form of a thick and dense band using 0.1 mM IPTG concentration and four hours of induction time as previously reported (Karamitros and Labrou, 2014). Stable gene expression exhibiting significant levels of asparaginase was observed because of the analysis which has also been reported previously on *Pseudomonas fluorescens* (Kishore *et al.*, 2015). The thermostable protein was partially purified by optimized heat treatment at 80 °C for 15 min and further purified by Ni-NTA chromatography as previously reported for purification of thermophilic L-asparaginase from *Thermococcus kodakarensis* where optimized heat treatment of 65°C for 30 min was used (Hong *et al.*, 2014).

Thermostable L-asparaginases are important components for mitigating the acrylamide content in processed foods by inhibiting the Maillard reaction, which

causes acrylamide production when asparagine reacts with reducing sugars (Alam *et al*., 2018). Temperatures higher than 100 °C are required for this reaction to take place. The asparaginase-like domain of asparaginase from *M. jannaschii* showed thermostability up to 90°C, which can be a potential candidate for its industrial applications. Further activity assays need to be optimized for the application studies.

DECLARATIONS

Ethical statement

The research work does not involve human or animal sampling and it was approved by the institutional Board of Advanced Studies and Research.

Informed consent statement

The information utilized in this research paper is public access and was appropriately cited for recognition of the original authors. Specific, informed consent was not deemed necessary.

Statement of conflict of interest

The authors have declared no conflict of interest.

REFERENCES

Alam, S., Ahmad, R., Pranaw, K., Mishra, P. and Khare, S.K., 2018. Asparaginase conjugated magnetic nanoparticles used for reducing acrylamide formation in food model system. *Bioresour. Technol*., **269**: 121-126. https://doi.org/10.1016/j.biortech.2018.08.095

Arif, S., Akhtar, M., Shad, M. and Akhtar, M.W., 2022. Recombinant production of MTB antigens and their purification by affinity chromatography. *Pak. J. Biochem. mol. Biol*., **55**: 226-231.

Bansal, S., Gnaneswari, D., Mishra, P. and Kundu, B., 2010. Structural stability and functional analysis of L-asparaginase from *Pyrococcus furiosus*. *Biochemistry* (Moscow), **75**: 375-381. https://doi.org/10.1134/S0006297910030144

Chi, H., Jiang, Q., Feng, Y., Zhang, G., Wang, Y., Zhu, P., Lu, Z. and Lu, F., 2023. Thermal stability enhancement of L-asparaginase from *Corynebacterium glutamicum* based on a semi-rational design and its effect on acrylamide mitigation capacity in biscuits. *Foods*, **12**: 4364. https://doi.org/10.3390/foods12234364

Chi, H., Wang, Y., Xia, B., Zhou, Y., Lu, Z., Lu, F. and Zhu, P., 2022. Enhanced thermostability and molecular insights for l-asparaginase from *Bacillus licheniformis* via structure-and computation-based rational design. *J. Agric. Fd. Chem*., **70**: 14499-14509. https://doi.org/10.1021/acs.jafc.2c05712

Chohan, S.M. and Rashid, N. 2018. Gene cloning and characterization ofrecombinant L-asparaginase from *Bacillus subtilis* strain R5. *Biologia,* **73**: 537-543. https://doi.org/10.2478/s11756-018-0054-1

Chohan, S.M., Rashid, N., Sajed, M. and Imanaka, T., 2019. Pcal_0970: An extremely thermostable L-asparaginase from *Pyrobaculum calidifontis* with no detectable glutaminase activity. *Folia Microbiol*., **64**: 313-320. https://doi.org/10.1007/s12223-018-0656-6

Dobryakova, N., Zhdanov, D., Dumina, M., Aleksandrova, S., Pokrovskaya, M., Genin, A., Shishparenok, A., Zhgun, A. and Kudryashova, E.V., 2023. Thermal inactivation mechanism and structural features providing enhanced thermal stability of hyperthermophilic *Thermococcus sibiricus* L-asparaginase in comparison with mesophilic and thermophilic L-asparaginases. *Catalysts*, **13**: 832. https://doi.org/10.3390/catal13050832

Dumina, M., Zhdanov, D., Zhgun, A., Pokrovskaya, M., Aleksandrova, S., Veselovsky, A. and El'darov, M., 2023. Enhancing the catalytic activity of thermo-asparaginase from Thermococcus sibiricus by a double mesophilic-like mutation in the substrate-binding region. *Int. J. mol. Sci*., **24**: 9632. https://doi.org/10.3390/ijms24119632

Dumina, M. and Zhgun, A., 2023. Thermo-l-asparaginases: From the role in the viability of thermophiles and hyperthermophiles at high temperatures to a molecular understanding of their thermoactivity and thermostability. *Int. J. mol. Sci*., **24**: 2674. https://doi.org/10.3390/ijms24032674

Farias, S.T. and Bonato, M., 2003. Preferred amino acids and thermostability. *Genet. Mol. Res*., **2**: 383-393.

Gabriel, M., Telmer, P.G. and Marsolais, F., 2012. Role of asparaginase variable loop at the carboxyl terminal of the alpha subunit in the determination

of substrate preference in plants. *Planta*, **235**: 1013-1022. https://doi.org/10.1007/s00425-011-1557-y

Hong, S.J., Lee, Y.H., Khan, A.R., Ullah, I., Lee, C., Park, C.K. and Shin, J.H., 2014. Cloning, expression, and characterization of thermophilic L-asparaginase from *Thermococcus kodakarensis kod1*. *J. Basic Microbiol*., **54**: 500-508. https://doi.org/10.1002/jobm.201300741

Javaid, S., Z. Ashi, A. Anwar, M. Akhter, S. Arif, M. Shad, M.W. Akhtar and M. Sajjad, 2022. Recombinant production and validation of immunogenic fragment from RBD of SARS-CoV-2 spike protein. *Pak. J. Biochem. mol. Biol*., **55**: 138-145.

Karamitros, C.S. and Labrou, N.E., 2014. Extracellular expression and affinity purification of L-asparaginase from *E. chrysanthemi* in *E. coli*. *Sustain. Chem. Process*., **2**: 1-8. https://doi.org/10.1186/s40508-014-0016-z

Kishore, V., Nishita, K. and Manonmani, H., 2015. Cloning, expression and characterization of L-asparaginase from *Pseudomonas fluorescens* for large scale production in *E. coli* BL21. *3 Biotech*, **5**: 975-981. https://doi.org/10.1007/s13205-015-0300-y

Li, J., Wang, J. and Bachas, L.G., 2002. Biosensor for asparagine using a thermostable recombinant asparaginase from *Archaeoglobus fulgidus*. *Anal. Chem*., **74**: 3336-3341. https://doi.org/10.1021/ac015653s

Li, X., Zhang, X., Xu, S., Zhang, H., Xu, M., Yang, T., Wang, L., Qian, H., Zhang, H. and Fang, H., 2018. Simultaneous cell disruption and semi-quantitative activity assays for high-throughput screening of thermostable L-asparaginases. *Sci. Rep*., **8**: 7915. https://doi.org/10.1038/s41598-018-26241-7

Loch, J.I. and Jaskolski, M., 2021. Structural and biophysical aspects of L-asparaginases: A growing family with amazing diversity. *Int. Union Crystallogr. J.,* **8**: 514-531. https://doi.org/10.1107/S2052252521006011

Lubkowski, J. and Wlodawer, A., 2021. Structural and biochemical properties of L-asparaginase. *FEBS J*., **288**: 4183-4209. https://doi.org/10.1111/febs.16042

Malandrin, L., Huber, H. and Bernander, R., 1999. Nucleoid structure and partition in *Methanococcus jannaschii*: An archaeon with multiple copies of the chromosome. *Genetics*, **152**: 1315-1323. https://doi.org/10.1093/genetics/152.4.1315

Munir, N., Zia, M.A., Sharif, S., Tahir, I.M., Jahangeer, M., Javed, I., Riaz, M., Sarwar, M.U., Akram, M.

and Shah, S.M.A., 2019. L-asparaginase potential in Acrylamide mitigation from foodstuff: A mini-review. *Prog. Nutr*., **21**: 498-506.

Nadeem, M., Khan, J., Al-Ghamdi, M., Khan, M. and Zeyadi, M., 2021. Studies on the recombinant production and anticancer activity of thermostable L-asparaginase i from *Pyrococcus abyssi*. *Braz. J. Biol*., **82**: e244735. https://doi.org/10.1590/1519-6984.244735

Naz, H., Gull, S., Bashir, Q., Rashid, N. and Shahzad, N., 2021. *Thermococcus kodakarensis*-derived L-asparaginase: A candidate for the treatment of glioblastoma. *Biologia*, **76**: 1305-1314. https://doi.org/10.2478/s11756-021-00678-0

Panja, A.S., Bandopadhyay, B. and Maiti, S., 2015. Protein thermostability is owing to their preferences to non-polar smaller volume amino acids, variations in residual physico-chemical properties and more salt-bridges. *PLoS One*, **10**: e0131495. https://doi.org/10.1371/journal.pone.0131495

Saeed, H., Hemida, A., El-Nikhely, N., Abdel-Fattah, M., Shalaby, M., Hussein, A., Eldoksh, A., Ataya, F., Aly, N. and Labrou, N., 2020. Highly efficient *Pyrococcus furiosus* recombinant L-asparaginase with no glutaminase activity: Expression, purification, functional characterization, and cytotoxicity on THP-1, A549 and Caco-2 cell lines. *Int. J. Biol. Macromol*., **156**: 812-828. https://doi.org/10.1016/j.ijbiomac.2020.04.080

Sajed, M., Falak, S., Muhammad, M.A., Ahmad, N. and Rashid, N., 2022. A plant-type L-asparaginase from *Pyrobaculum calidifontis* undergoes temperature dependent autocleavage. *Biologia*, **77**: 3623-3631. https://doi.org/10.1007/s11756-022-01215-3

Shad, M., Sajjad, M., Gardner, Q.A., Ahmad, S. and Akhtar, M.W., 2024. Structural engineering and truncation of α-amylase from the hyperthermophilic archaeon *Methanocaldococcus jannaschii*. *Int. J. Biol. Macromol*., **256**: 128387. https://doi.org/10.1016/j.ijbiomac.2023.128387

Shad, M., Usman, M. and Gardner, Q.A., 2023. Structural-functional characterization of cytochrome b in bc1 and b6 f complexes along with polymorphic analysis. *Pakistan J. Zool*., **55**: 975-986. https://doi.org/10.17582/journal.pjz/20220428110433

Shad, M., Hussain, N., Usman, M., Akhtar, M.W. and Sajjad, M., 2023. Exploration of computational approaches to predict the structural features and recent trends in α-amylase production for industrial applications. *Biotechnol. Bioeng*., **120**: 2092-2116. https://doi.org/10.1002/bit.28504

Susanti, D., Frazier, M.C. and Mukhopadhyay, B., 2019. A genetic system for *Methanocaldococcus jannaschii*: An evolutionary deeply rooted hyperthermophilic methanarchaeon. *Front. Microbiol.*, **10**: 1256. https://doi.org/10.3389/fmicb.2019.01256

Yao, M., Yasutake, Y., Morita, H. and Tanaka, I., 2005. Structure of the type-I L-asparaginase from the hyperthermophilic archaeon *Pyrococcus horikoshii* at 2.16 Å resolution. *Acta Crystallogr. D: Biol. Crystallogr.,* **61**: 294-301. https://doi.org/10.1107/S0907444904032950

Zielezinski, A., Loch, J.I., Karlowski, W.M. and Jaskolski, M., 2022. Massive annotation of bacterial L-asparaginases reveals their puzzling distribution and frequent gene transfer events. *Sci. Rep.*, **12**: 15797. https://doi.org/10.1038/s41598-022-19689-1

Zuo, S., Xue, D., Zhang, T., Jiang, B. and Mu, W., 2014. Biochemical characterization of an extremely thermostable L-asparaginase from *Thermococcus gammatolerans ej3*. *J. Mol. Catal. B Enzymat.*, **109**: 122-129. https://doi.org/10.1016/j.molcatb.2014.08.021

Zuo, S., Zhang, T., Jiang, B. and Mu, W., 2015. Reduction of acrylamide level through blanching with treatment by an extremely thermostable L-asparaginase during french fries processing. *Extremophiles*, **19**: 841-851. https://doi.org/10.1007/s00792-015-0763-0